FULL PAPER *Internal Medicine*

A Clinical Study on Velocity Patterns of Pulmonary Venous Flow in Canine Heartworm Disease

Takeshi SHIBATA, Yoshito WAKAO and Mitsugi TAKAHASHI

Department of Veterinary Surgery, School of Veterinary Medicine, Azabu University, 1–17–71 Fuchinobe, Sagamihara, Kanagawa 229–8501, Japan

(Received 12 August 1999/Accepted 1 November 1999)

ABSTRACT. In this study, we evaluated methods of determining the velocity patterns of pulmonary venous flow (PVF) in dogs and then investigated the relationship of the patterns to cardiac functions in heartworm disease (HD) by transthoracic echocardiography (TTE). The results revealed that there was a good correlation between PVF patterns determined by transesophageal echocardiography (TEE) and TTE in animals lying on their left sides. The measurement of S and D wave velocities (PVS and PVD) by TTE was shown to allow clinical determination of the velocity patterns of PVF in dogs. The HD groups showed significant increases in PVS and PVD, and S and D wave time-velocity integrals (S-TVI and D-TVI) of the right cranial lobe PVF, when compared with the normal group, as determined by TTE ($P<0.05$). In contrast, the HD groups produced significant decreases in PVD and D-TVI of the right caudal lobe PVF compared with the normal group ($P<0.05$), and a significant increase in the ratio of S-TVI to (S-TVI + D-TVI) ($P<0.05$). It is, therefore, suggested that measurement of the velocity patterns of the right cranial and caudal lobe PVF could be one method of assessing the stages of obstructive lesions in the pulmonary artery.—KEY WORDS: canine, canine heartworm disease, pulmonary venous flow, transesophageal echocardiography, transthoracic echocardiography.

J. Vet. Med. Sci. 62(2): 169–177, 2000

Dogs with heartworm disease (HD) will have pulmonary hypertension associated with pulmonary embolism caused by dead heartworms or increased pulmonary vascular resistance induced by proliferative lesions in the intima and media of the pulmonary artery caused by the irritation of heartworms [2, 3, 5, 7, 8, 13, 14, 18–20]. Two arterial systems form the pulmonary circulation: one is the pulmonary artery, by which gas exchange occurs across the alveolus, and the other is the bronchoesophageal artery (BE-A), which plays a primary role in nutritional blood supply to the lungs. Obstrution of the pulmonary peripheral blood flow could be compensated by the dilatation or proliferation of the BE-A through the formation of a broncho-pulmonary (B-P) shunt [10, 15, 24]. Consequently, the number of heartworms or their dead bodies could initiate the development of the compensatory proliferation of BE-A following pulmonary embolism or pulmonary proliferative lesions, resulting in various changes in the parameters of pulmonary venous circulation.

The transesophageal echocardiography (TEE) for human clinical use is applicable to observation of the velocity patterns of pulmonary venous flow (PVF) in dogs. However, when holding animals in a fixed position or introducing a transesophageal probe into their esophagus, they need to be given a general anesthesia, which may adversely affect the velocity patterns of PVF or cardiac functions. Moreover, such a method is not always easy to use in a clinical setting. Conversely, a transthoracic wall approach without anesthesia may have advantages for the observation of the velocity pattern of PVF by Doppler echocardiography in dogs [1, 9]. In the present study, we have, therefore, attempted to establish a method of observing the velocity patterns of PVF by transthoracic echocardiography (TTE), and compared it with TEE. The present study, furthermore, was designed to investigate the relationship between the velocity patterns of PVF and cardiac functions in HD dogs using TTE, focusing on the changes in these parameters due to B-P shunt associated with heartworms, in order to clarify the hemodynamics of pulmonary circulation of the HD dogs.

MATERIALS AND METHODS

Experiment I. Comparison of the velocity patterns of PVF determined by TEE and TTE

Animals: Five beagles (mean weight of 9.9 ± 3.3 kg) and 9 mongrel adult dogs (mean weight of 12.1 ± 1.1 kg), who had no abnormal findings of chest and hemodynamics, were selected for the study following chest radiography, microfilaria detection, auscultation, ECG, phonocardiology, and echography.

Experimental procedures: Dogs were given 25 mg/kg i.v. of thiopental sodium (Ravonal®) for anesthesic induction 15 min after premedication with 0.025 mg/kg s.c. of atropine sulfate, and kept anesthetized by inhalation of fluothane (Halothane®) (oxygen-fluothane anesthesia), maintained at an anesthetic concentration of 1–1.5%. The animals lying on their backs, underwent TEE to determine the velocity patterns of PVF. The same animals were then held on their left sides and received both TEE and TTE to identify the velocity pattern of PVF. The velocity patterns of PVF were determined using a sector electronic scanning ultrasonic tomography apparatus (EUB-565A; Hitachi Medical Corporation) through a bi-plane type transducer (7.5 MHz;

Hitachi Medical Corporation) for TEE, and an electro sector type transducer (5 MHz; Hitachi Medical Corporation) for TTE.

Measurement procedures: Animals, held lying on their backs, underwent TEE to obtain the velocity patterns of PVF, the right cranial and caudal lobe PVF and left ventricular inflow. The velocity pattern of PVF was determined by locating the transducer at the site at which the mitral image is generated, drawing the probe up in the esophagus. Likewise, the velocity patterns of the cranial and caudal lobe PVF were determined by generating their color Doppler images from the inflow velocity signal into the left atrium. The velocity pattern of left ventricular inflow was measured at the site at which the mitral image is generated by moving the transducer to its proper place.

The sample volume was set at the left atrial orifice of the pulmonary artery for identifying the velocity patterns of cranial and caudal lobe PVF, and at the mitral annulus for left ventricular inflow. The velocity patterns of cranial and caudal lobe PVF were measured for S and D wave velocities (PVS and PVD) and heart rate (HR); if a split PVS consisting of S_1 and S_2 waves (PVS_1 and PVS_2), was generated, the velocity of the faster component was referred to as that of PVS. The velocity patterns of left ventricular inflow were measured for E and A waves (VE and VA) and heart rate (HR). Each of the measurements were expressed as the mean value of 4 waves.

Subsequently, the animals, held lying on their left sides, underwent both TEE and TTE to obtain the velocity pattern. The TEE was performed in the same way as in the animals on their backs. The velocity patterns of cranial and caudal lobe PVF were determined by creating a color Doppler image, on the left ventricular long-axis view based on the left apex approach, from the inflow velocity signal into the left atrium. The velocity pattern of left ventricular inflow was obtained on the left ventricular long-axis view based on the left apex approach. The sample volume was set at the same site as that used for the animals on their backs. The velocity patterns of cranial and caudal lobe PVF and left ventricular inflow were measured using the same parameters as those used for the animals held on their backs. In the present study, using TEE and TTE, the confluent velocity patterns of right cranial and middle lobe PVF are referred to as the right cranial lobe PVF, and right caudal and accessory lobe PVF.

Experiment II. Changes in the velocity pattern of PVF and cardiac functions of HD dogs

Animals: Five adult beagles (mean weight of 9.7 ± 1.6 kg), who had no abnormal findings in the same examinations as those described in Experiment I. were selected for the normal group. Fourteen mongrel adult dogs (mean weight of 11.2 ± 1.2 kg), who were diagnosed with HD, based on a positive reading in microfilaria test and bulge in the pulmonary arterial trunk and right and left pulmonary arteries detected by the chest radiography, were selected for the HD groups. The HD group was divided into two groups, "the mild HD group" and "the advanced HD group",

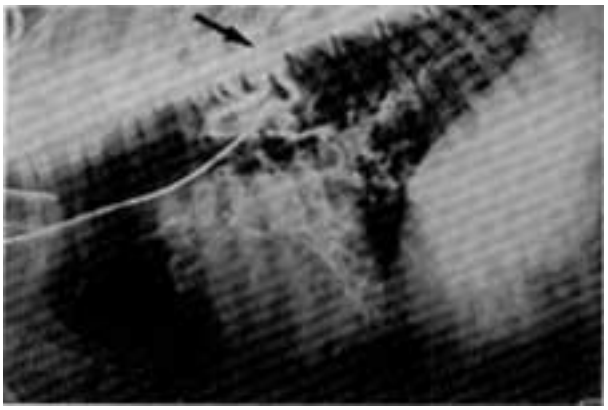

Fig. 1. Selected angiogram of bronchoesophageal artery (BE-A) and aorta in the advanced HD group. BE-A is dilated at ramification (arrow), showing the ratio of BE-A to aorta diameters to be 0.25 or more.

according to whether the BE-A had developed to a mild extent, or to a moderate or high extent (Fig. 1).

Experimental procedures: Dogs were given the same anesthesia as described in Experiment I. in Materials and Methods. After their left external carotid artery and jugular vein were separated, we performed an angiography of BE-A by injecting an iodic contrast medium (ISOPEKU®) through a catheter, whose tip was thinned and inserted into the left external carotid artery. A bolus injection of the contrast medium was consistently given in a volume of 3 m*l* to avoid a variation in the diameter of BE-A, which various injection rates or volumes could induce. The catheter was then pulled back so that its tip could be placed in the aortic arch, and 5 m*l* of the contrast medium was injected via the catheter to perform an angiography of the aorta. The tips of two catheters, which were set through the left external carotid artery and jugular vein, were placed in the left ventricle and pulmonary artery by the aid of radiography to measure left ventricular and pulmonary arterial pressures, respectively.

A sector electronic scanning ultrasonic tomography apparatus (EUB-165; Hitachi Medical Corporation) was used along with a sector type (7.5 MHz, EUP-S33; Hitachi Medical Corporation) and steerable transducers (2.5 MHz, EUP-SD300A; Hitachi Medical Corporation) for Doppler echocardiography in the normal and HD groups. Animals were fixed on their left sides and TTE or PD was performed via a 2.5 MHz transducer to determine the velocity patterns of PVF and left ventricular inflow, aortic flow and right ventricular inflow as measurements of cardiac function. The animals in the HD groups showing right ventricular regurgitation underwent measurement of the velocity pattern of regurgitant flow by continuous wave (CW) Doppler via a 2.5 MHz transducer. Animals were subjected to TTE, lying on their right sides to measure the velocity pattern of pulmonary arterial flow (PAF) via a 2.5 MHz transducer. Furthermore, the animals showing PAF regurgitation

underwent measurement of the velocity pattern of regurgitant flow by CW Doppler via a 2.5 MHz transducer. A 7.5 MHz probe was used to measure left ventricular structures and eccentricity ratio by M-mode echocardiography.

Measurement procedures: The diameters of BE-A and aorta were determined by measuring them in ramus bronchoesophagica on the angiogram via radiography with a pair of calipers. Left intraventricular and pulmonary arterial pressures were determined with pressure transducers connected to catheters whose tips were placed in the left ventricle and pulmonary artery, and recorded on a polygraph. An analysis of the averaged wave patterns in nine consecutive waves was made with an ECG processor (Softoron Co.). The velocity patterns of PVF (right cranial and caudal PVF) and left ventricular inflow were measured by the same method as that described in Experiment I. Moreover, the velocity patterns of aortic flow and right inflow were measured on an apical 4-chamber view of the heart. The sample volume was set at the aortic and tricuspid orifices. The animals lying on their right sides were subjected to TTE to obtain the velocity pattern of PAF, which created a short-axis view (aortic valval level) based on a right-thoracic approach and set sample volume at the pulmonary valval orifice. Each of the measurements were expressed as the mean value of 4 consecutive waves. The same animals underwent M-mode echocardiography to determine the parameters of heart structure on a left ventricular short-axis view (papillary muscle level) based on a right-thoracic approach. Each of the measurements were expressed as the mean value of 3 consecutive waves. The distance (A) between interventricular septum and posterior papillary muscles of the left ventricle was determined on a left ventricular short-axis view (papillary muscle level) based on a right-thoracic approach by M-mode echocardiography. Likewise, the maximum short-axis diameter (B) of the left intraventricular cavity, which made a right angle to the view for A was measured to obtain the ratio of left ventricular diameters (B/A) referred to as the eccentricity ratio. The ratio of the left atrial diameter to aortic diameter (LA/Ao) was obtained from the measurements on a left ventricular short-axis view (papillary muscle level) based on a parasternal approach by M-mode echocardiography.

Statistical analysis: Mann-Whitney U test, paired t-test, one way analysis of variance, and Kruskal-Wallis test were performed using the measurement data of the respective groups. A valve of $P<0.05$ or 0.01 was considered significant.

RESULTS

Experiment I. Comparison of the velocity patterns of PVF determined by TEE and TTE

(1) Correlation among the velocity patterns of PVF and left ventricular inflow and body positions determined by TEE

VA, PVS and PVD which were measured by TEE were generated clearly in a laminar flow pattern. There were animals that showed a split PVS, each of which consisted of PVS_1 and PVS_2. Each of the animals underwent TEE to determine the velocity patterns of the right cranial and caudal PVF and left ventricular inflow, in turn on their back and left sides. There was a negative correlation between PVS of right cranial lobe PVF in animals lying on their backs and left sides (correlation coefficient: $r=-0.778$). Conversely, there was a poor correlation between the respective flow velocities other than PVS measured in both body positions: $r=0.449$ for PVD of right cranial lobe PVF, $r=0.486$ and 0.348 for PVS and PVD of right caudal lobe PVF. A positive correlation was well observed between VE and VA of left ventricular inflow ($r=0.789$) and the ratio of VA to VE (A/E) ($r=0.863$) in animals lying on their backs and left sides, but the correlation coefficient for VA was as low as 0.551.

(2) Correlation of the velocity patterns of PVF and left ventricular inflow determined by TEE and TTE

The velocity patterns of PVF by TEE consisted of VA, PVS and PVD, which were generated clearly in a laminar flow pattern. PVS and PVD were both created clearly by TTE and their waves in many animals were in a laminar flow pattern. This was possibly because the animals' respiration and holding were both well controlled as a result of anesthesia. However, there was difficulty in clearly generating VA in certain animals.

Each of the animals were subjected in turn to TEE and TTE to determine the velocity patterns of the right cranial and caudal PVF and left ventricular inflow while lying on the left side. A positive correlation was well observed for PVS and PVD of the right cranial lobe PVF ($r=0.944$ for PVS, $r=0.903$ for PVD), and the velocity patterns of the right caudal lobe PVF ($r=0.799$ for PVS, $r=0.848$ for PVD) between the measurements made by TEE and TTE (Figs. 2, 3). Likewise, a positive correlation was well observed for VE and VA of the left ventricular inflow ($r=0.914$ for VE, $r=0.774$ for VA), and the ratio of A/E ($r=0.882$) between both echocardiography methods.

Experiment II. Changes in the velocity pattern of PVF and cardiac functions in HD dogs

The measurement of PVF and cardiac functions in normal dogs and HD dogs are summarized in Table 1.

(1) Changes in the velocity patterns of right cranial and caudal lobe PVF

When measuring the velocity patterns of the right cranial lobe PVF in the normal and HD groups by TTE, there was a significant increase in PVS in the mild HD group compared with the normal group, and in the advanced HD group compared with the mild HD group ($P<0.05$). In PVD, there was a significant increase in the advanced HD group compared with the normal group. Likewise, a significant increase in the advanced HD group, when compared with the normal group, was observed for both S and D wave time-velocity integrals (S-TVI and D-TVI) ($P<0.05$) (Figs. 4, 5, 6).

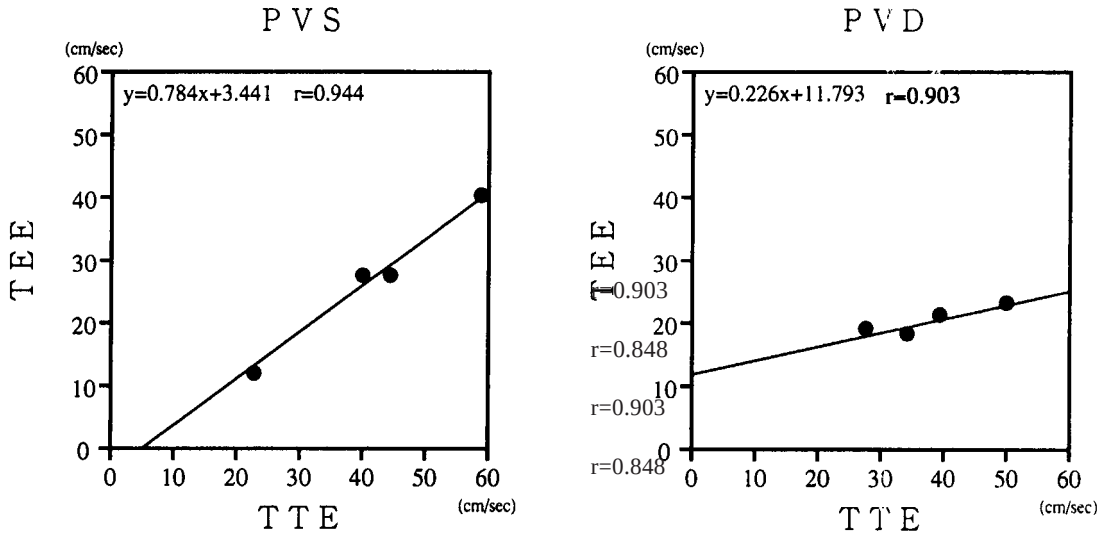

Fig. 2. Correlation of the velocity pattern of right cranial lobe PVF determined by transesophageal (TEE) and transthoracic echocardiography (TTE). There were close correlations in PVS and PVD: PVS, S wave flow velocity; PVD, D wave flow velocity.

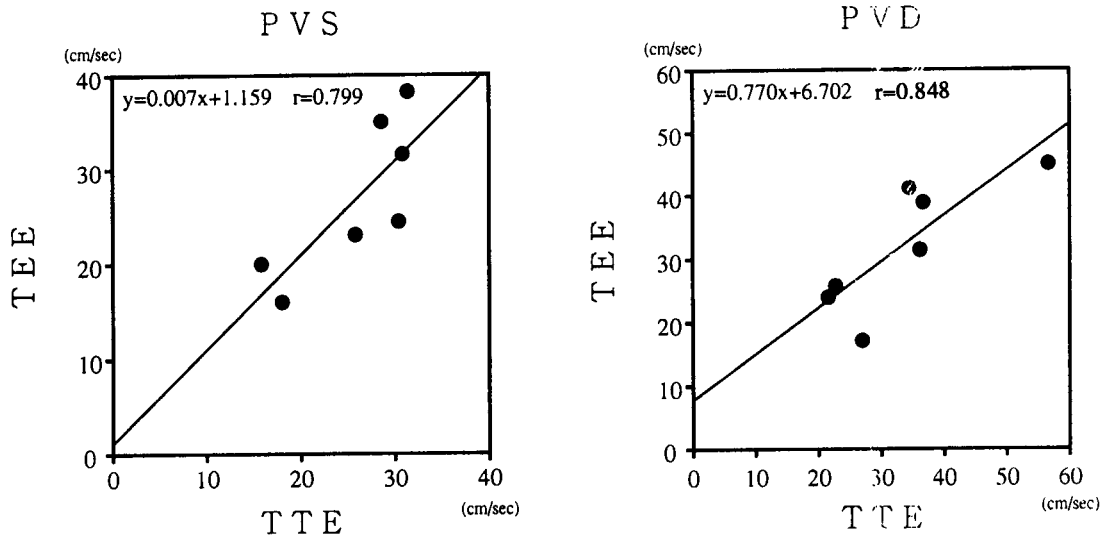

Fig. 3. Correlation of the velocity patterns of right caudal lobe PVF determined by TEE and TTE. There were close correlations in PVS and PVD.

There were no significant differences in PVS among the three groups for measurements of the velocity pattern of the right caudal lobe PVF in the normal and HD groups. However, there was a significant decrease in PVD in the advanced HD group compared with the normal group ($P<0.05$). There were no significant differences in S-TVI among the three groups, but there was a significant decrease for D-TVI in the advanced HD group compared with the normal group ($P<0.05$) (Figs. 7, 8). A significant increase in the advanced HD group, when compared with the normal group, was also observed for the ratio of S-TVI to (S-TVI+D-TVI) (Ts/(Ts+Td)) ($P<0.05$).

(2) Changes in left heart function

Significant increases in A/E wave flow velocities in the mild and advanced HD groups, compared with the normal group ($P<0.01$), were observed in measurements of the left ventricular functions in the normal and HD groups by the TTE. An increase in mean aortic blood flow was observed in the advanced HD group compared with the normal group. At the same time, there was an elevation in the eccentricity ratio (B/A) during the diastolic phase in the normal group while there was a trend to fall in the mild and advanced HD groups, both of which showed slightly deformed left ventricles based on radiography.

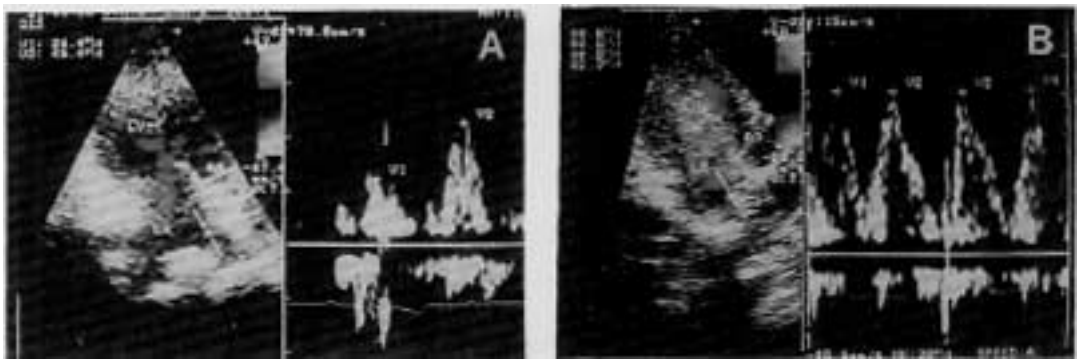

Fig. 4. Waveforms of right cranial lobe PVF determined by TTE. A, normal group; B, advanced HD group. In the advanced HD group, the increased height of PVS (V1) and PVD (V2) is seen. LA, Left atrium; LV, Left ventricle; AO, Aorta.

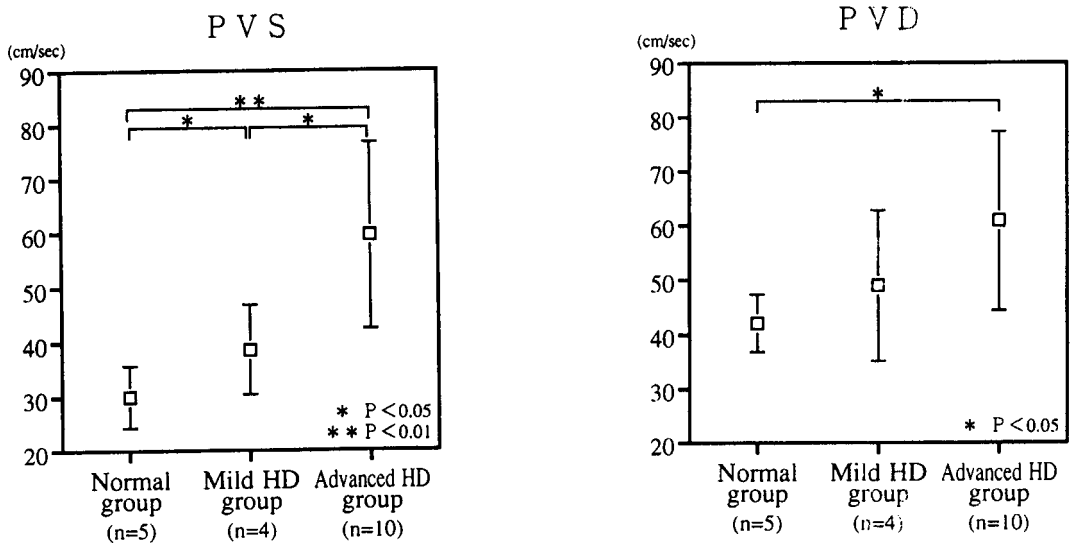

Fig. 5. The velocity pattern of right cranial lobe PVF in the normal, mild and advanced HD groups. Increased PVS and PVD were observed in the advanced HD groups, and there was a significant difference between the normal and the advanced HD groups.

(3) Changes in right heart function

There was a significant decrease in acceleration time (AT) of the velocity of the right ventricular inflow in the advanced HD group compared with the normal group ($P<0.05$). There was also a significant increase in acceleration (Acc) of PAF velocity in the advanced HD group compared with that of the normal group ($P<0.05$), and a significant decrease in AT and the ratio of AT to ejection time (AT/ET) of the right ventricular inflow compared with the normal group ($P<0.05$). Moreover, based on the pressure difference, which was calculated from the peak velocity of regurgitant flow at the tricuspid valve, determined by the TTE, a significant elevation in right intraventricular pressure was observed in the HD groups compared with the normal group ($P<0.05$).

DISCUSSION

It has been reported that obstructive lesions in the pulmonary artery of HD dogs are observed in the right caudal lobe of the lung [7]. Moreover, a synthetic resin cast preparation of the pulmonary artery indicates that many lesions would occur in the right caudal lobe of the lung in HD [23]. The impaired pulmonary arterial circulation leads to proliferation of BE-A. A markedly proliferated BE-A in the right caudal lobe of the lung was also observed in our angiogram of the artery. The BE-A in normal animals originates from the aorta, intercostal and internal thoracic arteries, and extends to the bronchium, pulmonary artery and vein, producing a netty structure covering their surfaces for nutritional supply [15]. About one third of BE-A blood flow runs into the left atrium through the short BE-A and

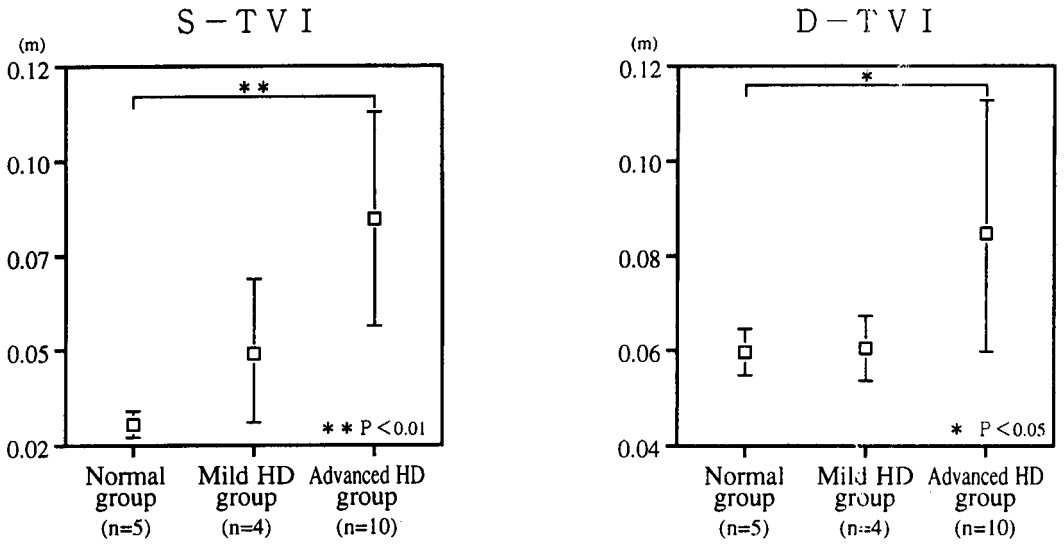

Fig. 6. Time-velocity integral (TVI) of right cranial lobe PVF in the normal, mild and advanced HD groups. Increased S- and D-TVIs were observed in the HD groups, and there was a significant difference between the normal and advanced HD groups: S-TVI, S wave time-velocity integral; D-TVI, D wave time-velocity integral.

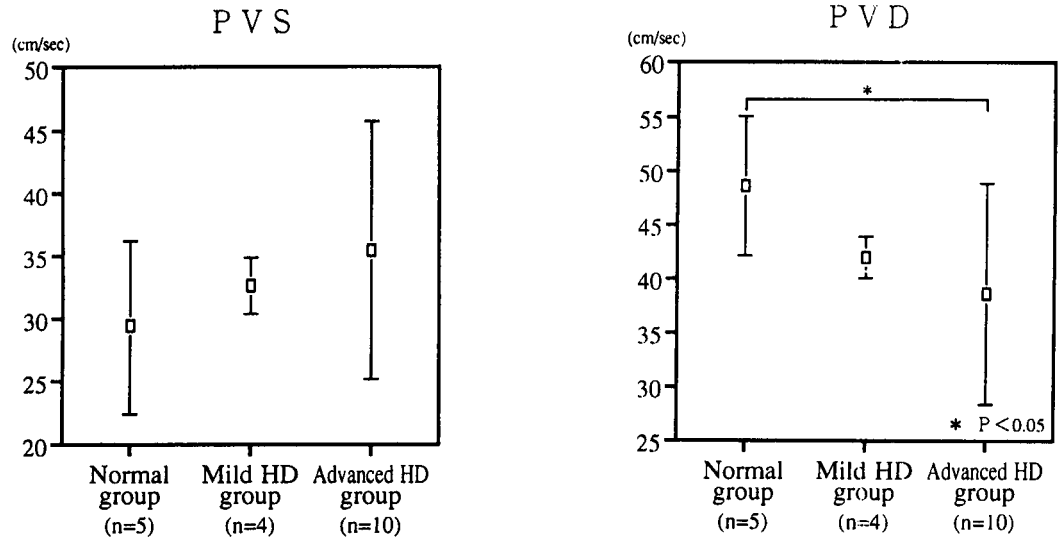

Fig. 7. The velocity patterns of right caudal lobe PVF in the normal, mild and advanced HD groups. Increased PVS was observed in the HD groups, but there was no significant difference from the normal group. A decreased PVD was observed, with a significant difference between the normal and the advanced HD groups.

pulmonary vein, and the rest of the blood flows into the right atrium through the azygos vein after passing through bronchoesophageal vein [15]. Moreover, it has been suggested that the BE-A blood runs directly into the pulmonary artery via precapillary anastomoses [21]. In contrast with normal animals, the obstructed flow of peripheral pulmonary blood could be compensated for with blood flow through precapillary anastomoses (B-P shunt) formed between the bronchoesophageal and pulmonary arteries in ischemic lung parenchyma and pulmonary arterial circulatory disorders associated with HD [11, 24].

Therefore, impaired circulation associated with obstructive lesions in pulmonary artery presumably affects the outflow from the lungs, for example in PVF. Furthermore, the dilatation, proliferation or B-P shunt formation of BE-A may allow much blood in the aorta to flow into the pulmonary vein, affecting pulmonary venous circulation.

Many studies have reported the factors determining the waveform in VA, PVS or PVD and the effects of various cardiac diseases and aging on the flow velocity in pulmonary vein were determined by Doppler echocardiography [12,

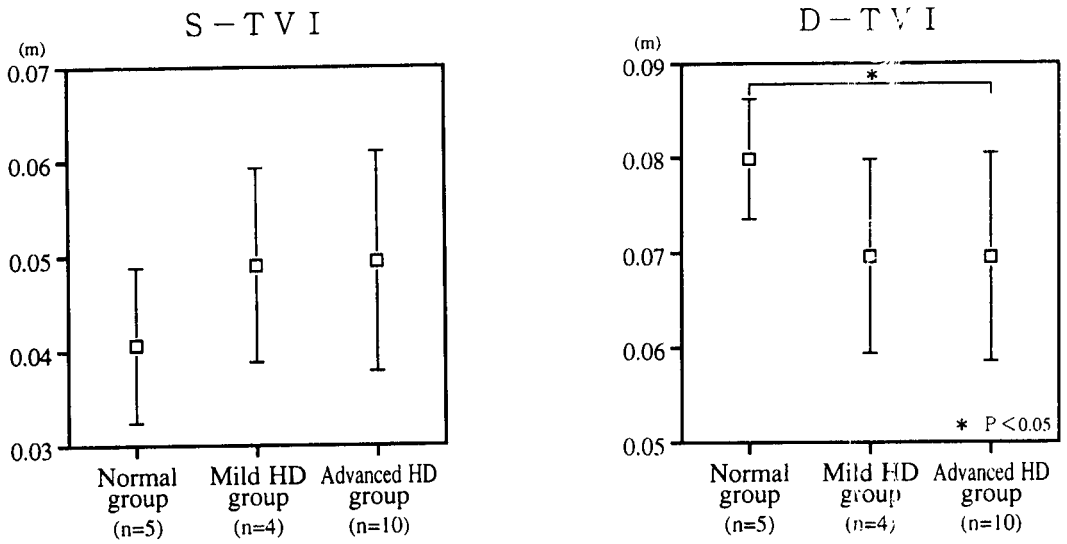

Fig. 8. Time-velocity integral (TVI) of right caudal lobe PVF in the normal, mild and advanced HD groups. Increased S-TVI was observed in the HD groups, but with no significant difference from the normal group. A decreased D-TVI was observed, with a significant difference between the normal and advanced HD groups.

16,17]. However, the effects of lung lesions on the velocity patterns of PVF have been hardly reported in the areas of veterinary and human medicine. In the present study, we have, therefore, attempted to estimate the changes in the hemodynamics of the lung in HD, focusing on the effects of HD on the velocity pattern of PVF measured by Doppler echocardiography.

There was no correlation between PVS or PVD in animals lying on their backs and left sides by TEE. Conversely, there was a definite correlation for VA and VD determined by TEE and TTE in animals lying on their left sides. Although TTE was able to generate neither VA, PVS_1 nor PVS_2 Doppler images of PVF clearly, it provided PVS and PVD patterns with out the most reliability. Since the velocity pattern of PVF by TEE was difficult to determine in the supine position, the animals underwent echocardiography lying on their left sides, allowing us to compare the velocity pattern of PVF measured by both echocardiography methods. Thus, the velocity patterns of left and right heart flow velocities as well as those of the right cranial and caudal lobe PVF could be determined by TTE. The HD group was divided into two groups according to the degree of BE-A proliferation to determine the velocity patterns of right cranial and caudal lobe PVF in each group. The results indicate that venous return to the left atrium in the HD groups was greater than that in the normal group. As the stages of pulmonary embolism or obstructive lesions associated with retained dead heartworms in the pulmonary artery advances, the blood flow of the pulmonary artery will be disturbed and furthermore obstructed in the areas of the lung with severe lesions. This will likely result in a decrease in PVF coming from the right caudal lobe, which has severe lesions. However, the HD groups showed increases in PVS, PVD, S- and D-TVIs in right cranial lobe PVF compared with the normal group, indicating that blood return to the pulmonary vein increased through B-P shunts.

When comparing the velocity patterns of PVF in the HD groups, PVS of the right cranial lobe PVF in the advanced HD group was greater than that in the mild HD group, but no significant differences in PVD and D-TVI were found between the HD groups. There was no significant differences in PVS and PVD of the right caudal lobe PVF between both HD groups. The present results suggest that the progression of obstructive lesions in the right caudal lobe of the lung led to increased vascular resistance of the pulmonary artery, which most likely resulted in the greater PVS in the right cranial lobe PVF. Furthermore, the high velocity value of the right caudal lobe PVF was possibly due to an increased BE-A flow into the lung area of the lesion. Therefore, the velocity patterns of the right cranial and caudal lobe PVF could represent parameters for estimating progression of obstructive lesions in the pulmonary artery associated with HD.

The data on cardiac functions by Doppler echocardiography suggests that HD dogs displayed a tendency of decreasing diastolic function of the left ventricle. The high ratio of VA to VE in left ventricular inflow indicates an increased left ventricular inflow that was driven by the contracted left atrium as a result of the disturbed rapid filling function at the end diastole. The disturbed rapid filling function at the end diastole may be explained by impaired diastolic function of the left ventricle associated with the interventricular septum pressing in the direction of the left ventricle due to an enlarged right ventricle, because HD animals have shown decreased compliance of interventricular septum due to its increased thickness [4]. Moreover, the eccentricity ratio was of a high value in the present study. It has been reported that

Table 1. Measurement of pulmonary venous flow and cardiac functions in normal dogs and heartworm disease dogs

		Normal group (n=5)		Mild HD group (n=4)		Advanced HD group (n=10)	
		Mean ± SD	Range	Mean ± SD	Range	Mean ± SD	Range
Right cranial lobe PVF	PVS (cm/s)	29.6±5.5	24.5to38.0	39.1±8.9	26.9to46.5	59.3±17.0	42.6to92.6
	PVD (cm/s)	42.7±4.8	38.7to50.6	48.5±12.3	31.1to57.4	60.4±16.1	39.0to91.1
	S-TVI (m)	0.03±0.004	0.03to0.04	0.05±0.02	0.02to0.06	0.08±0.03	0.05to0.15
	D-TVI (m)	0.06±0.01	0.05to0.06	0.06±0.01	0.05to0.07	0.09±0.03	0.05to0.13
	HR(beats/min)	106.8±29.1	75to139	110.5±19.7	83to127	104.8±20.6	75to130
Right caudal lobe PVF	PVS (cm/s)	29.2±6.3	23.2to39.0	33.0±1.9	30.1to34.2	36.1±9.9	27.7to61.3
	PVD (cm/s)	49.1±7.7	40.0to60.9	42.7±2.7	40.7to46.4	38.8±6.7	30.7to50.6
	S-TVI (m)	0.04±0.001	0.03to0.06	0.05±0.01	0.04to0.07	0.05±0.01	0.04to0.07
	D-TVI (m)	0.08±0.01	0.07to0.09	0.07±0.01	0.05to0.07	0.07±0.01	0.05to0.09
	HR(beats/min)	107.8±27.8	68to145	106.5±17.3	86to126	104.4±17.5	78to122
Left ventricular inflow	VE (cm/s)	64.7±16.4	47.7to90.4	51.2±5.1	46.6to58.5	48.4±8.1	36.1to60.8
	VA (cm/s)	46.1±10.1	36.3to61.9	53.2±5.6	47.6to59.4	52.5±6.9	43.7to70.1
	A/E	0.70	0.51to0.88	1.04	0.84to1.17	1.10	0.81to1.46
	AT (m/s)	51.9±5.7	43.0to57.0	60.5±15.2	47.8to82.3	55.2±14.8	38.0to90.0
	ET (m/s)	394.6±140.2	201to581	298.5±62.1	257to391	343.6±129.0	200to658
	HR (beats/min)	102.0±28.5	76to149	112.0±16.2	90to129	101.1±19.6	63to139
Aortic flow	Vp (cm/s)	114.6±15.7	99.1to138.0	99.1±2.21	95.9to101.0	99.8±19.0	71.8to145.0
	Vm (cm/s)	77.2±8.4	66.0to88.3	66.9±1.3	65.3to68.0	65.9±10.9	55.0to92.7
	AT (m/s)	39.0±5.9	33.0to48.0	442.3±5.0	37.0to47.0	44.1±10.5	31.0to64.0
	ET (m/s)	173.2±20.0	143to193	167±8.8	159to178	181.5±12.1	170to203
	AT/ET	0.22	0.17to0.29	0.25	0.21to0.29	0.24	0.17to0.35
	Acc (m/s^2)	30.9±7.4	21.5to39.8	25.3±3.9	21.5to29.9	24.1±7.1	11.4to32.7
	TVI (m)	0.13±0.01	0.11to0.14	0.11±0.1	0.11to0.12	0.12±0.02	0.09to0.16
	HR (beats/min)	88.4±18.8	79to122	109.5±13.0	91to120	95.1±18.2	63to111
Right inflow	VE (cm/s)	39.1±8.3	27.9to49.4	42.9±5.6	37.5to50.5	45.2±10.4	35.8to71.8
	VA (cm/s)	43.3±11.5	31.6to61.0	55.3±11.0	44.0to66.6	52.3±9.0	43.4to75.0
	A/E	1.11	0.78to1.23	1.29	1.01to1.55	1.17	0.92to1.43
	AT (m/s)	87.6±32.7	57to138	91.7±12.3	75.5to105.0	62.9±14.3	41to85
	ET (m/s)	383±111.6	247to558	328.5±38.9	279to374	374.8±133.5	231to655
	HR (beats/min)	103.8±20.7	79to136	112.8±11.4	99to127	100.2±23.6	67to120
Pulumonary arterial flow	Vp (cm/s)	106.4±18.7	85.8to137.0	89.8±17.0	65.8to106.0	104.2±24.3	84.5to148.0
	Vm (cm/s)	73.1±12.9	58.2to93.3	61.0±11.0	45.6to71.5	69.1±14.6	53.9to101.0
	AT (m/s)	81.3±20.1	43.8to100.0	71.9±24.8	37.0to95.5	50.8±15.3	31.8to70.7
	ET (m/s)	195.0±29.9	162to228	182.8±23.7	165to215	183.9±14.7	168to213
	AT/ET	0.41	0.29to0.54	0.39	0.22to0.51	0.25	0.06to0.41
	Acc (m/s^2)	14.2±4.9	8.6to21.5	15.0±9.64	8.38to29.2	23.2±7.0	12.0to31.5
	TVI (m)	0.14±0.02	0.12to0.16	0.11±0.01	0.09to0.12	0.13±0.03	0.10to0.18
	HR (beats/min)	105.6±29.0	81to152	118.8±17.0	97to138	108.9±12.2	83to126

PVF=pulmonary venous flow; PVS=peak velocity of systolic flow; PVD=peak velocity of diastolic flow; S-TVI=time-velocity integral of systolic flow; D-TVI=time-velocity integral of diastolic flow; VE=peak velocity of early diastolic filling flow; VA=peak velocity of late diastolic filling flow; AT=acceleration time; ET=ejection time; Vp=peak velocity; Vm=mean velocity; Acc=acceleration; HR=heart rate.

the impaired diastolic function of the left ventricle in HD produced a high end diastolic pressure [6, 22], but the present study did not corroborate these findings. This may be primarily explained by an inhibited circulatory function through inhalation anesthesia with halothane in HD dogs displaying disturbed pulmonary circulation.

Obstructive lesions in the pulmonary artery associated with proliferated intima and medium of the artery are considered to be the main causes of the development of pulmonary hypertension in HD dogs. Wakao *et al.* [23] have reported that the flow in the BE-A, which proliferates as the stages of HD advance, had an effect on pulmonary hypertension as one of the parameters for its development. In the report, the authors view that the occlusion or enhancement of BE-A inflow produced a decrease or increase in pulmonary arterial pressure, respectively, suggesting that BE-A flow directly affects pulmonary arterial pressure, promoting the development of pulmonary hypertension.

The present study indicates that left ventricular functions

in the HD groups were depressed compared with the normal group, but no great difference in left atrial venous return or left ventricular functions was found between the mild and advanced HD groups, between which there is a difference in extent of BE-A development caused by pulmonary obstructive lesions. Therefore, it is suggested that the decreased left atrial venous return in HD dogs was compensated by venous return through increased BE-A flow. Furthermore, the systemic circulation was considered to have no significant variation in blood flow between the mild and advanced HD groups because there was no great difference in left ventricular functions between the groups. The present results suggest that compensatory blood flow in BE-A promotes pulmonary hypertension developing with a progression of obstructive lesions in the pulmonary artery through its return into the peripheral pulmonary arterial and venous systems.

REFERENCES

1. Chiang, C.H., Hagio, M., Yoshida, H. and Okano, S. 1998. Pulmonary venous flow in normal dogs recorded by transthoracic echocardiography: Techniques, anatomic validations and flow characteristics. *Jpn. J. Vet. Sci.* 60: 333–339.
2. Clarence, R.A. 1980. Acute response of pulmonary blood flow and right ventricular function to dirofilaria immitis adults and microfilaria. *Am. J. Vet. Res.* 41: 244–249.
3. Crissman, R.S. and Ross, J. N. Jr. 1983. Electron microscopy of intimial lesions in the pulmonary trunk of a dog with dirofilaria immitis. *J. Submicrosc. Cytol.* 15: 509–517.
4. Fishman, A.P. 1958. The "effective" pulmonary collateral blood flow in man. *J. Clin. Invest.* 37: 1071–1085.
5. Hennigar, G.R. and Ferguson, R.W. 1957. Plumonary vascular sclerosis as a result of dirofilaria immitis infection in dogs. *J. Am. Vet. Med. Assoc.* 121: 336–341.
6. Henry, W.M. 1955. Magnitude and time of development of the collateral circulation to the lung after occlusion of the left pulmonary artery. *Circ. Res.* 111: 422–424.
7. Jerry, A.L. 1961. Pulmonary arterial lesions in canine dirofilariasis. *Am. J. Vet. Res.* 22: 655–662.
8. Keith, J.C., Schaub, R.G. and Rawlings, C.A. 1983. Early arterial injury induced myointimal proliferation in canine pulmonary arteries. *Am. J. Vet. Res.* 44: 181–186.
9. Kerens, Gad. 1985. Pulmonary venous flow pattern—its relationship to cardiac dynamics. *Circulation* 71: 1105–1112.
10. Kobayashi, K., Nakayama, M. and Kato, R. 1988. Acute lung disorders and bronchial circulation. *Jan. J. Thorac. Dis.* 26: 341–346.
11. Kotani, T., Tomimura, T. and Mochizuki, H. 1976. Pathological study of pulmonary circulation disorders associated with heartworm disease by postmortem angiography. *Jpn. J. Vet. Sci.* 38: 459–511.
12. Kuecherer, H.F. 1990. Estimation of mean left atrial pressure from transesophageal pulsed Doppler echocardiography pulmonary vein flow. *Circulation* 82: 1127–1139.
13. Kume, S., Yamanaka, M., Kariya, T. and Tabe, A. 1982. Metabolic systems in platelet and thrombogenesis. *Jpn. J. Clin. Med.* 40: 683–694.
14. Munnell, J.F., Weldom, J.S., Lewis, R.E., Thrall, D.E. and Call, J.W.M. 1980. Intimal lesions of the pulmonary artery in dogs with experimental Dirofilariasis. *Am. J. Vet. Res.* 41: 1108–1112.
15. Murata, K., Ito, S. and Todo, Y. 1984. Angioarchitectonics in bronchial arterial circulation. *Jpn. J. Clin. Rad.* 29: 941–948.
16. Ogawa, S. 1990. Estimation of factors determining systolic waveform in the velocity pattern of pulmonary venous flow. *In the proceeding of the Japan Society of Ultrasonic in Medicine.* 57: 329–330.
17. Rick, N.A. 1990. Relation of pulmonary vein to mitral flow velocities by transesophageal doppler echocardiography. *Circulation* 81: 1488–1497.
18. Schaub, R.G. and Rawlings, C.A. 1980. Pulmonary vascular response during phases of canine hertworm disease: Scanning electron microscopic study. *Am. J. Vet. Res.* 41: 1082–1089.
19. Schaub, R.G., Keith, J.C. and Rawlings, C.A. 1983. Effect of acetylsalicylic acid on vascular damage and myointimal proliferation in canine pulmonary arteries subjected to chronic injury by dirofilaria immitis. *Am. J. Vet. Res.* 44: 449–454.
20. Schaub, R.G., Rawlings, C.A. and Keith, J.C.Jr. 1981. Platelet adhesion and myointimal proliferation in canine pulmonary arteries. *Am. Assoc. Pathol.* 104: 13–22.
21. Szidon, J.P., Ingram, R.H. and Fishaman, A.P. 1968. Origin of the pulmonary venous flow pulse. *Am. J. Physiol.* 214: 10–14.
22. Takemura, N. 1989. Changes in canine cardiac functions associated with heartworm in pulmonary artery. *J. Vet. Med. Sci.* 42: 771–773.
23. Wakao, Y., Okumura, A., Ninomiya, H. and Takahashi M. 1992. Cause of canine pulmonary hypertension associated with heartworm disease—Effect of proliferation of bronchoesophageal artery on pulmonary artery. *Jpn. J. Electrocardiol.* 12: 134–141.
24. Jintoku, H. 1957. Morphological study of pulmonary vascular system 1. Changes in pulmonary vascular system in lycopodium lung embolism. *Jpn. J. Const. Med.* 22: 39–45.